

Cite this: *Chem. Sci.*, 2019, 10, 3242

All publication charges for this article have been paid for by the Royal Society of Chemistry

Received 14th November 2018  
Accepted 3rd February 2019

DOI: 10.1039/c8sc05063e

rsc.li/chemical-science

# Nickel-catalyzed oxidative C–H/N–H annulation of *N*-heteroaromatic compounds with alkynes†

Atsushi Obata, Akane Sasagawa, Ken Yamazaki, Yusuke Ano and Naoto Chatani \*

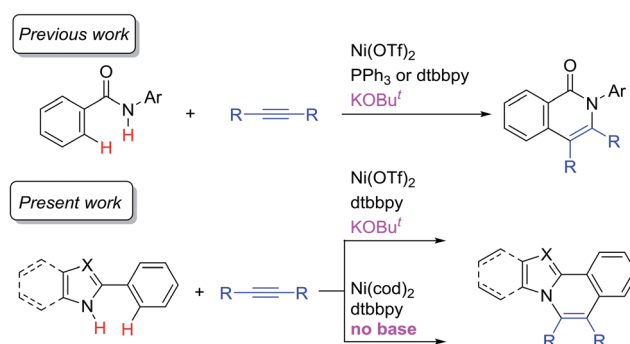
The reaction of *N*-heteroaromatic compounds, such as 2-aryl-pyrrole, benzimidazole, imidazole, indole, and pyrazole derivatives, with alkynes in the presence of a catalytic amount of a nickel complex results in C–H/N–H oxidative annulation. The reaction shows a high functional group compatibility. While both Ni(0) and Ni(II) complexes show a high catalytic activity, Ni(0) is proposed as a key catalytic species in the main catalytic cycle. In the case of the Ni(II) system, the presence of a catalytic amount of a strong base, such as KOBu<sup>t</sup>, is required for the reaction to proceed. In sharp contrast, a base is not required in the case of the Ni(0) system. The proposed mechanism is supported by DFT studies.

## Introduction

Transition-metal catalyzed C–H functionalization reactions have experienced notable progress over the past two decades.<sup>1</sup> At the early stage of the development of such reactions, noble metals, such as Pd, Rh, Ir, and Ru, were frequently used as catalysts and these metals continue to be the catalysts of choice in various C–H functionalization reactions. However, the use of first row transition metals,<sup>2</sup> such as Fe,<sup>3</sup> Co,<sup>4</sup> Ni,<sup>5</sup> and Cu,<sup>6</sup> has attracted a great deal of interest because they are earth-abundant and therefore less expensive than noble metals. If these elements could be used in such transformations, it would permit the scope of C–H functionalization reactions to be greatly expanded. Among these metals, nickel catalysts are of particular interest. Although a pioneering example of cyclo-metalation with the cleavage of an *ortho* C–H bond was achieved by the reaction of azobenzene with a nickel complex,<sup>7</sup> Ni-catalyzed C–H functionalization reactions have generally remained undeveloped. One of the reasons for this is the absence of a general and reliable catalytic system for Ni-catalyzed C–H functionalization. In fact, Ni-catalyzed C–H functionalization reactions were limited to specific substrates that contain an acidic C–H bond, such as pentafluorobenzene, pyridine derivatives, and azoles.<sup>5a</sup> However, since our initial report in 2013 on the use of an 8-aminoquinoline directing group<sup>8</sup> in Ni(II)-catalyzed C–H alkylation with alkyl halides,<sup>9a</sup> a combination of Ni(II) catalysts and *N,N'*-bidentate directing groups has now emerged as a powerful methodology for use in Ni-catalyzed C–H functionalization reactions.<sup>5b,c</sup> Since then, the Ni(II) catalyst/8-aminoquinoline directing system has been

extensively used for the development of Ni-catalyzed C–H functionalizations.<sup>5b,c,9,10</sup>

In a previous study, we reported on the Ni-catalyzed oxidative annulation of C–H bonds in aromatic amides with alkynes, leading to the production of 1(2*H*)-isoquinolinones (Scheme 1).<sup>11</sup> In this reaction, a specific *N,N'*-bidentate directing group is not required for the reaction to proceed, in contrast to our study in 2011.<sup>12</sup> A key to the success of the reaction is the use of a catalytic amount of KOBu<sup>t</sup>. We wish to report herein that this newly developed system is also applicable to the oxidative annulation of C–H bonds in various 2-aryl-*N*-heteroaromatic compounds (Scheme 1). A theoretical study was also conducted in connection with these experimental findings. The DFT studies indicated that the reaction proceeds *via* two reaction paths. One mechanism is initiated by Ni(II) and KOBu<sup>t</sup>, and the other, the main catalytic cycle, is initiated by Ni(0). Although the Ni(II) system requires a base, the Ni(0) system proceeds even in the absence of KOBu<sup>t</sup>. Nitrogen-containing polyaromatic scaffolds are widely found in natural products, pharmaceutical agents, and  $\pi$ -conjugated functional materials.<sup>13</sup> A similar transformation was previously reported using noble metal



Scheme 1 Ni-catalyzed oxidative C–H/N–H annulation of *N*-heteroaromatic compounds with alkynes.

Department of Applied Chemistry, Faculty of Engineering, Osaka University, Suita, Osaka 565-0871, Japan. E-mail: chatani@chem.eng.osaka-u.ac.jp

† Electronic supplementary information (ESI) available. CCDC 1868340. For ESI and crystallographic data in CIF or other electronic format see DOI: 10.1039/c8sc05063e



complexes, such as  $[\text{Cp}^*\text{RhCl}_2]_2$  and  $[\text{RuCl}_2(p\text{-cymene})]_2$ .<sup>14</sup> The present reaction is the first example of the use of a nickel catalyst in oxidative C–H/N–H annulation reactions with alkynes.

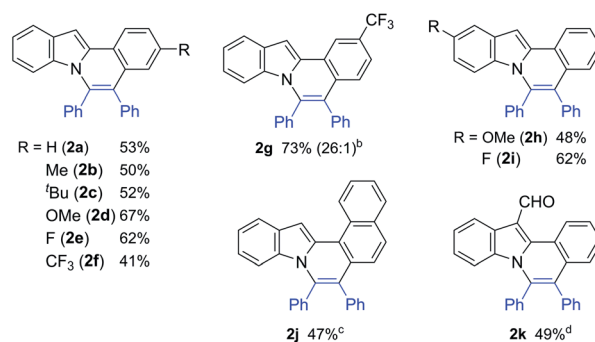
## Results and discussion

The reaction of 2-phenylindole (**1a**) with diphenylacetylene was carried out under the same reaction conditions as were used in the reaction of aromatic amides.<sup>11a</sup> Unexpectedly, no reaction took place (entry 1 in Table 1). However, the use of 4,4-di-*tert*-butyl-2,2-dipyridyl (dtbbpy) as a ligand in place of  $\text{PPh}_3$  gave the expected product, 5,6-diphenylindolo[2,1-*a*]isoquinoline (**2a**) (entry 2). Increasing the reaction temperature to 180 °C slightly improved the product yield (entry 3). Conducting the reaction in the absence of a solvent resulted in a further improvement in the product yield (entry 4). Finally, the reaction conditions shown in entry 5 were used as standard reaction conditions. Curiously,  $\text{Ni}(\text{cod})_2$  also showed catalytic activity (entry 6). This result will be discussed below in relation to the reaction mechanism.

The scope of this oxidative annulation reaction with respect to 2-arylindole derivatives was also investigated (Table 2). A variety of functional groups, including methoxy, fluoride, trifluoromethyl, and even formyl groups, were tolerated in the reaction. In the reaction of 3-trifluoromethylphenylindole (**2g**), the less hindered C–H bond was selectively activated. In all cases, the yields of the expected product determined by <sup>1</sup>H NMR were good to high. However, a small amount of an unidentified product was produced as a contaminant. To remove this contaminant from the expected products, the product was purified by Gel Permeation Chromatography (GPC), which reduced the product yield.

To expand the present protocol, the reaction of 2-phenylbenzimidazole (**3a**) with diphenylacetylene was examined under

Table 2 Scope of 2-arylindoles<sup>a</sup>



<sup>a</sup> Reaction conditions: 2-arylindole (0.25 mmol), diphenylacetylene (1.25 mmol),  $\text{Ni}(\text{OTf})_2$  (0.025 mmol), dtbbpy (0.05 mmol), and  $\text{KO}^t\text{Bu}$  (0.05 mmol) at 180 °C for 36 h. Isolated by GPC. <sup>b</sup> The number in parentheses refers to the regioselectivity. <sup>c</sup> The reaction was carried out for 60 h. <sup>d</sup> Ligand (50 mol%) and toluene (0.25 mL).

Table 3 Ni-catalyzed reaction of 2-phenylimidazole (**3a**) with diphenylacetylene

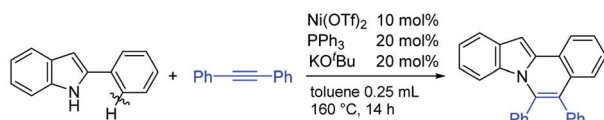


Entry	Catalyst	Notes	NMR yields	
			4a	3a
1	$\text{Ni}(\text{OTf})_2$		~100% (88%) <sup>a</sup>	0%
2	$\text{Ni}(\text{OAc})_2$		56%	0%
3	$\text{Ni}(\text{acac})_2$		33%	42%
4	$\text{NiCl}_2$		34%	39%
5	$\text{NiCp}_2$		28%	54%
6	$\text{Ni}(\text{cod})_2$		72%	0%
7	$\text{Ni}(\text{OAc})_2$	20 h	89%	0%
8	$\text{Ni}(\text{OAc})_2$	20 h, w/o $\text{KO}^t\text{Bu}$	6%	65%
9	$\text{Ni}(\text{OAc})_2$	20 h, toluene 0.5 mL	97%	0%
10	$\text{Ni}(\text{OAc})_2$	20 h, toluene 0.5 mL, 140 °C	51%	46%
11	$\text{Ni}(\text{OAc})_2$	20 h, phen, toluene 0.5 mL	87%	0%
12	$\text{Ni}(\text{OAc})_2$	20 h, bpy, toluene 0.5 mL	46%	26%

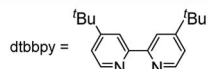


<sup>a</sup> Isolated yield.

Table 1 Ni-catalyzed reaction of 2-phenylindole (**1a**) with diphenylacetylene



Entry	Deviation for the standard conditions	NMR yields	
		2a	1a <sup>b</sup>
1	–	Trace	76%
2	dtbbpy	19%	n.d.
3	dtbbpy, 180 °C	30%	61%
4	dtbbpy, no solvent, 180 °C	51%	n.d.
5	dtbbpy, no solvent, 180 °C, 36 h	85% (53%) <sup>a</sup>	n.d.
6	$\text{Ni}(\text{cod})_2$ , dtbbpy, no solvent, 180 °C, 36 h	57%	n.d.



<sup>a</sup> Isolated by GPC. <sup>b</sup> n.d. = not determined.

the same reaction conditions as were used in the reaction of 2-phenylindole (Table 3). As expected, the corresponding product, 5,6-diphenylbenzo[4,5]imidazo[2,1-*a*]isoquinoline (**4a**), was formed in nearly quantitative yield (entry 1). A screening of various nickel salts indicated that other  $\text{Ni}(\text{II})$  complexes also showed catalytic activity (entries 2–5). Curiously,  $\text{Ni}(\text{cod})_2$  again showed a high catalytic activity (entry 6). We then decided to optimize the reaction conditions using  $\text{Ni}(\text{OAc})_2$  because  $\text{Ni}(\text{OTf})_2$  is prepared from  $\text{Ni}(\text{OAc})_2$  and trifluoromethanesulfonic acid in  $\text{CH}_3\text{CN}$ ,<sup>9a</sup> and is sensitive to moisture and air. The use of a longer reaction time resulted in an increased product yield (entry 7). In the absence of  $\text{KO}^t\text{Bu}$ ,



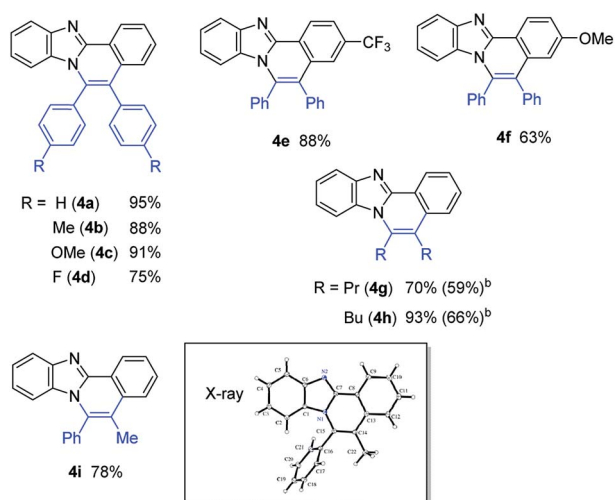
the product yield was dramatically decreased (entry 8). The use of phenanthroline (phen) also gave **4a** in high yield (entry 11), but the use of the bipyridine (bpy) ligand did not lead to optimal yields (entry 12). Finally, we determined that the reaction conditions shown in entry 9 are standard reaction conditions for the reaction of 2-phenylimidazole with alkynes.

With the optimized reaction conditions in hand, we examined the scope of 2-arylimidazoles **3** and alkynes (Table 4). Not only diarylalkynes, but also aliphatic alkynes were applicable to the reaction. The reaction of **3** with aliphatic internal alkynes gave the corresponding benzo[4,5]imidazo[2,1-*a*]isoquinoline derivatives **4g** and **4h** in high yields. The reaction of **3** with phenylpropyne gave the corresponding product **4i** in a regioselective manner, the structure of which was confirmed by X-ray crystallographic analysis.

The reaction of 2-phenylimidazole (**5**), 3,5-diphenylpyrazole (**7**), and 2-phenylpyrrole (**9**) also gave the corresponding nitrogen-containing polyaromatic compounds, **6**, **8**, and **10**, respectively (Table 5).

To gain insights into the reaction mechanism, the reaction was carried out in the presence of two equivalents of TEMPO. However, TEMPO did not inhibit the reaction, indicating that a radical path is not involved in the catalytic system (Scheme 2). As shown in Tables 1 and 3, the catalytic activity of Ni(cod)<sub>2</sub> was comparable to that of Ni(II) complexes in the presence of KO<sup>t</sup>Bu. Curiously, it was found that the reaction proceeds in a highly efficient manner, even in the absence of KO<sup>t</sup>Bu. The reaction of **3a** without KO<sup>t</sup>Bu gave **4a** in a quantitative yield. Indole **1a** also gave **2a**. Thus, the use of KO<sup>t</sup>Bu is crucial for the reaction to proceed when Ni(II) complexes are used as a catalyst. In sharp contrast, KO<sup>t</sup>Bu is not required when Ni(0) is used as a catalyst. The reaction of **3a** with diphenylacetylene in the presence of Ni(cod)<sub>2</sub>/dtbbpy gave **4a** in 85% NMR yield, along with a 55%

Table 4 Ni-catalyzed reaction of 2-arylimidazoles (**3**) with alkynes<sup>a</sup>



<sup>a</sup> Reaction conditions: 2-arylimidazole (0.25 mmol), alkyne (1.25 mmol), Ni(OAc)<sub>2</sub> (0.025 mmol), dtbbpy (0.05 mmol), and KO<sup>t</sup>Bu (0.05 mmol) in toluene (0.5 mL) at 160 °C for 20 h. <sup>b</sup> The number in parentheses refers to the isolated yield by HPLC.

Table 5 Other *N*-heteroaromatic compounds



Scheme 2 Mechanistic experiments.

yield of stilbene relative to **4a**. In the absence of **3a**, no evidence was found for the formation of stilbene. These results indicate that diphenylacetylene functions as a hydrogen acceptor as well as a two-component coupling partner. A deuterium-labelling experiment in the absence of an alkyne was also carried out. H/D exchange took place only at the *ortho*-position.



Table 6 Ni(0)/no base catalytic system<sup>a</sup>

R = H ( <b>4a</b> ) 87%	R = OMe ( <b>4c</b> ) 81% <sup>b</sup>	<b>4i</b> 73%
CF <sub>3</sub> ( <b>4e</b> ) 83% <sup>b</sup>	F ( <b>4d</b> ) 76% <sup>b</sup>	
OMe ( <b>4f</b> ) 88% <sup>b</sup>		

<sup>a</sup> Reaction conditions: 2-arylimidazole (0.25 mmol), alkyne (1.25 mmol), Ni(cod)<sub>2</sub> (0.025 mmol), and dtbbpy (0.05 mmol) in toluene (0.5 mL) at 160 °C for 20 h. <sup>b</sup> 0.125 Mmol scale.

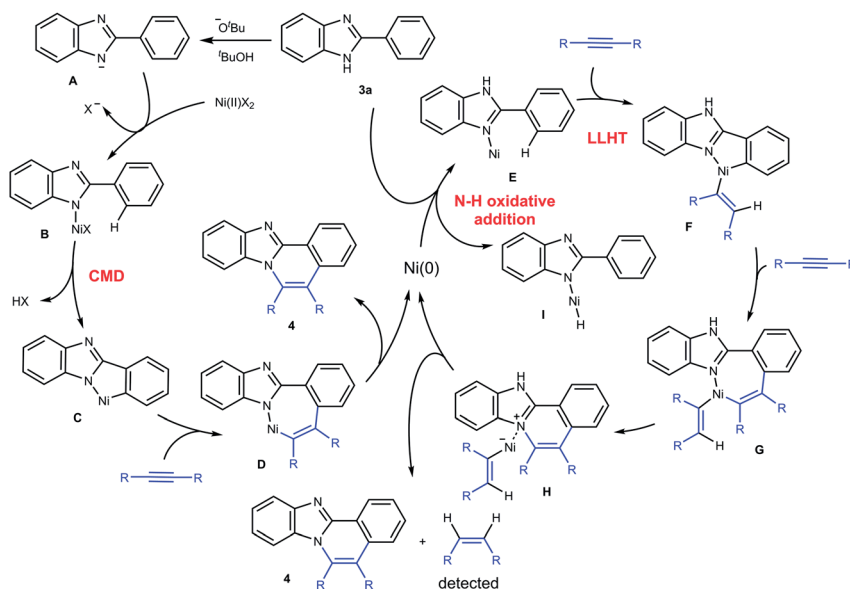
Some examples of the use of other substrates in the Ni(cod)<sub>2</sub>/no base system are summarized in Table 6.

Based on these results, a mechanism for the C–H/N–H oxidative annulation is proposed, as shown in Scheme 3. The mechanism involves two paths and is initiated by the Ni(II) complex (left scheme). An NH proton is abstracted from **3a** by KOBu<sup>t</sup> to generate the anion **A**, which reacts with Ni(II) to give the complex **B**. The cleavage of the *ortho* C–H bond followed by the insertion of an alkyne into a C–Ni bond in **C** gives complex **D**. A reductive elimination from **D** then gives **4a** and Ni(0). However, Ni(0) cannot be re-oxidized to Ni(II) to complete a catalytic cycle under the reaction conditions employed. Instead, Ni(0) initiates another catalytic cycle (right scheme). The coordination of a N(sp<sup>2</sup>) atom in **3a** to Ni(0) gives complex **E**, which involves a ligand-to-ligand hydrogen transfer (LLHT) mechanism,<sup>15,16</sup> in which the *ortho* hydrogen atom is directly transferred to the alkyne carbon. The successive insertion of an alkyne into C–Ni bonds gives the complex **G**. Reductive elimination followed by deprotonation affords **4a** with the regeneration of Ni(0) and the concomitant formation of an alkene. In fact, the formation of alkenes was detected by GC (Scheme 2).

An alternative mechanism involves the oxidative addition of a N–H bond in **3a** to Ni(0), leading to the generation of complex **I**. The possibility of this alternative mechanism being operative will be discussed below in conjunction with DFT studies.

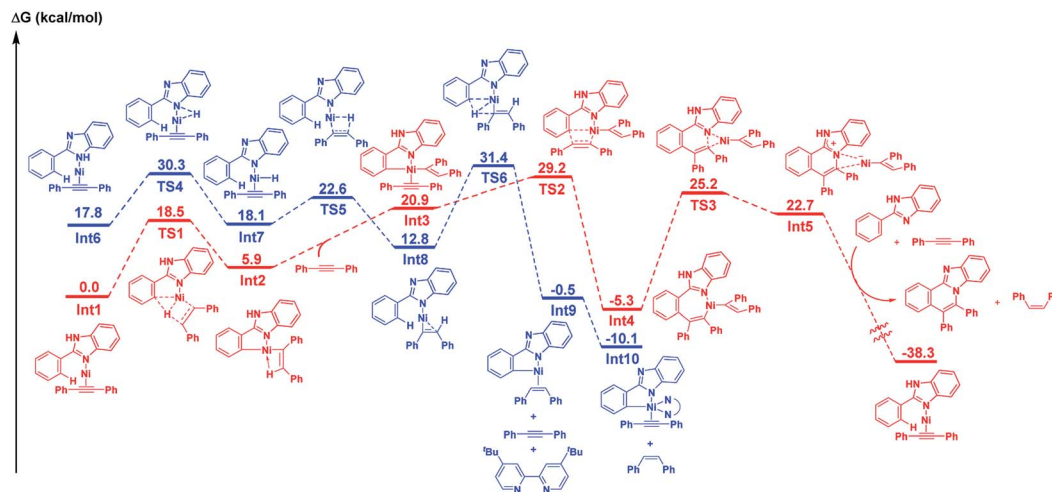
DFT studies were conducted in an attempt to obtain a better understanding of the mechanism for this reaction. The resulting DFT studies are essentially supportive of the mechanism that is proposed above. As shown by the mechanistic details in Scheme 3, the presence of KOBu<sup>t</sup> is crucial for the success of the initial reaction path (left scheme in Scheme 3), which is catalyzed by Ni(II), but it is not required for the main catalytic cycle in which Ni(0) functions as a catalyst (right scheme in Scheme 3). Therefore, we focused on the main reaction path that is initiated by Ni(0) under neutral conditions (red line in Scheme 4).<sup>17</sup> The LLHT mechanism for the main catalytic cycle that proceeds *via* **TS1** has a low energy barrier (18.5 kcal mol<sup>−1</sup>). After coordination with a second alkyne molecule, the insertion of the alkyne into a Ni–C bond through **TS2** proceeds smoothly, with an activation energy of 8.3 kcal mol<sup>−1</sup>. A final reductive elimination through **TS3** from the relatively stable seven-membered metallacycle **Int4** requires a large amount of energy to produce **Int5**, which is comprised of an ammonium cation and nickel anion pair. This step is followed by a proton shift to afford the product and the *cis*-alkene with the regeneration of **Int1**. While a detailed mechanism for the proton shift is not given here, the large amount of energy released during the course of the catalytic cycle is assumed to be the driving force for the reaction.

We also investigated the case where the main catalytic cycle is initiated by the oxidative addition of an N–H bond (complex **I** in Scheme 3 and the blue line in Scheme 4), because the presence of an N(sp<sup>2</sup>) atom in the substrate is not essential for the reaction to proceed, as in 2-phenylindole or pyrrole. The coordination of an N(sp<sup>2</sup>) atom to nickel, as in **Int6**, was found to be energetically unfavorable, compared with the coordination of



Scheme 3 Proposed mechanism.





Scheme 4 Comparison of the LLHT path (red line) and the N–H oxidative addition path (blue line) in the main catalytic cycle calculated at the B3PW91/6-311+G(2d,p)-SDD(Ni)/PCM//B3LYP/6-31+G(d)-LanL2dz(Ni) level of theory.

an  $N(sp^2)$  atom. While a LLHT path from the N–H bond of 2-phenylimidazole to an alkyne could not be located, the oxidative addition of the N–H bond in **Int6** through **TS4**, followed by the insertion of the alkyne into a Ni–H bond is a feasible step. The  $\sigma$ -bond metathesis through **TS6** proceeds with an activation energy of  $18.6 \text{ kcal mol}^{-1}$  to give a five membered metallacycle **Int9**. The highest Gibbs free energy for this step is the transition state of the  $\sigma$ -bond metathesis step ( $31.4 \text{ kcal mol}^{-1}$ ), which is slightly higher than that for the LLHT mechanism ( $29.2 \text{ kcal mol}^{-1}$ ). These results indicate that, while the reaction of 2-phenylimidazole proceeds through a LLHT mechanism, it is possible that the reaction of 2-phenylindole could proceed *via* the N–H oxidative addition- $\sigma$ -bond metathesis sequence.

## Conclusions

We report on the development of a new catalytic system for oxidative C–H/N–H annulation with alkynes which is promoted by a Ni(II)/KOBu<sup>t</sup> or Ni(0) system. Using this system it is possible to use N-heteroaromatic compounds, such as 2-aryl-pyrrole, benzimidazole, imidazole, indole, and pyrazole, in Ni-catalyzed oxidative C–H/N–H annulation reactions with alkynes, leading to the production of highly conjugated compounds. While noble metal complexes, such as  $[Cp^*RhCl_2]_2$  and  $[RuCl_2(p\text{-cymene})]_2$ , were used in the past in a similar transformation, the present reaction is the first example of the oxidative C–H/N–H annulation with alkynes in which a nickel catalyst is used. DFT studies indicate that the reaction involves two reaction paths. One mechanism is initiated by Ni(II) and the other by Ni(0), the latter being the main catalytic cycle. Although the Ni(II) system requires a base, the Ni(0) system proceeds, even in the absence of KOBu<sup>t</sup>. C–H activation in the first step proceeds through a CMD mechanism and C–H activation in the main catalytic cycle proceeds through a LLHT mechanism.

## Conflicts of interest

There are no conflicts to declare.

## Acknowledgements

This work was supported by a Grant-in-Aid for Specially Promoted Research by The Ministry of Education, Culture, Sports, Science and Technology (17H06091).

## Notes and references

- For reviews on C–H functionalization, see: (a) K. M. Engle, T.-S. Mei, M. Wasa and J.-Q. Yu, *Acc. Chem. Res.*, 2012, **45**, 788; (b) J. J. Mousseau and A. B. Charette, *Acc. Chem. Res.*, 2013, **46**, 412; (c) J. J. Topczewski and M. S. Sanford, *Chem. Sci.*, 2015, **6**, 70; (d) Z. Chen, B. Wang, J. Zhang, W. Yu, Z. Liu and Y. Zhang, *Org. Chem. Front.*, 2015, **2**, 1107; (e) L. Yang and H. Huang, *Chem. Rev.*, 2015, **115**, 3468; (f) J. Ye and M. Lautens, *Nat. Chem.*, 2015, **7**, 863; (g) J. F. Hartwig and M. A. Larsen, *ACS Cent. Sci.*, 2016, **2**, 281; (h) A. Dey, S. Agasti and D. Maiti, *Org. Biomol. Chem.*, 2016, **14**, 5440; (i) H. M. L. Davies and D. Morton, *ACS Cent. Sci.*, 2017, **3**, 936; (j) O. Baudoin, *Acc. Chem. Res.*, 2017, **50**, 1114; (k) L. Ping, D. S. Chung, J. Bouffard and S.-g. Lee, *Chem. Soc. Rev.*, 2017, **46**, 4299; (l) P. Nareddy, F. Jordan and M. Szostak, *ACS Catal.*, 2017, **7**, 5721; (m) C. G. Newton, S.-G. Wang, C. C. Oliveira and N. Cramer, *Chem. Rev.*, 2017, **117**, 8908; (n) J. R. Hummel, J. A. Boerth and J. A. Ellman, *Chem. Rev.*, 2017, **117**, 9163; (o) Y. Park, Y. Kim and S. Chang, *Chem. Rev.*, 2017, **117**, 9247; (p) K. Murakami, S. Yamada, T. Kaneda and K. Itami, *Chem. Rev.*, 2017, **117**, 9302; (q) Z. Dong, Z. Ren, S. J. Thompson, Y. Xu and G. Dong, *Chem. Rev.*, 2017, **117**, 9333; (r) M. P. Drapeau and L. J. Gooßen, *Chem.–Eur. J.*, 2016, **22**, 18654; (s) K. Hirano and M. Miura, *Chem. Sci.*, 2018, **9**, 22; (t) J. C. K. Chu and T. Rovis, *Angew. Chem., Int. Ed.*, 2018, **57**, 62; (u) S. Vásquez-Céspedes, X. Wang and F. Glorius, *ACS Catal.*, 2018, **8**, 242; (v) W.-J. Zhou, Y.-H. Zhang, Y.-Y. Gui, L. Sun and D.-G. Yu, *Synthesis*, 2018, **50**, 3359; (w) C. Sambigao, D. Schönbauer, R. Blicke, T. Dao-Huy,



- G. Pototschnig, P. Schaaf, T. Wiesinger, M. F. Zia, J. Wencel-Delord, T. Besset, B. U. W. Maes and M. Schnürch, *Chem. Soc. Rev.*, 2018, **47**, 6603; (x) Z. Zhang, P. H. Dixneuf and J.-F. Soule, *Chem. Commun.*, 2018, **54**, 7265; (y) E. N. da Silva Júnior, G. A. M. Jardim, R. S. Gomes, Y.-F. Liang and L. Ackermann, *Chem. Commun.*, 2018, **54**, 7398; (z) S. Rej and N. Chatani, *Angew. Chem., Int. Ed.*, 2018, DOI: 10.1002/anie.201808159.
- For recent reviews on direct functionalization of C–H bonds by first-row transition-metal catalysis, see: (a) J. Miao and H. Ge, *Eur. J. Org. Chem.*, 2015, 7859; (b) G. Pototschnig, N. Maulide and M. Schnürch, *Chem.–Eur. J.*, 2017, **23**, 9206.
  - For recent reviews on Fe-catalyzed C–H functionalization reactions, see: R. Shang, L. Ilies and E. Nakamura, *Chem. Rev.*, 2017, **117**, 9086.
  - For recent reviews on Co-catalyzed C–H functionalization reactions, see: (a) M. Moselage, J. Li and L. Ackermann, *ACS Catal.*, 2016, **6**, 498; (b) T. Yoshino and S. Matsunaga, *Adv. Synth. Catal.*, 2017, **359**, 1245; (c) Y. Kommagalla and N. Chatani, *Coord. Chem. Rev.*, 2017, **350**, 117; (d) S. Wang, S.-Y. Chen and X.-Q. Yu, *Chem. Commun.*, 2017, **53**, 3165.
  - For recent reviews on Ni-catalyzed C–H functionalization reactions, see: (a) J. Yamaguchi, K. Muto and K. Itami, *Eur. J. Org. Chem.*, 2013, 19; (b) L. C. Misal Castro and N. Chatani, *Chem. Lett.*, 2015, **44**, 410; (c) N. Chatani, *Top. Organomet. Chem.*, 2016, **56**, 19; (d) J. Yamaguchi, K. Muto and K. Itami, *Top. Curr. Chem.*, 2016, **374**, 55.
  - For recent reviews on Cu-catalyzed C–H functionalization reactions, see: (a) K. Hirano and M. Miura, *Chem. Lett.*, 2015, **44**, 868; (b) A. P. Jadhav, D. Ray, V. U. B. Rao and R. P. Singh, *Eur. J. Org. Chem.*, 2016, 2369; (c) J. Liu, G. Chen and Z. Tan, *Adv. Synth. Catal.*, 2016, **358**, 1174; (d) W.-H. Rao and B.-F. Shi, *Org. Chem. Front.*, 2016, **3**, 1028.
  - J. P. Kleiman and M. Dubeck, *J. Am. Chem. Soc.*, 1963, **85**, 1544.
  - V. G. Zaitsev, D. Shabashov and O. Daugulis, *J. Am. Chem. Soc.*, 2005, **127**, 13154.
  - (a) Y. Aihara and N. Chatani, *J. Am. Chem. Soc.*, 2013, **135**, 5308; (b) Y. Aihara and N. Chatani, *J. Am. Chem. Soc.*, 2014, **136**, 898; (c) Y. Aihara, M. Tobisu, Y. Fukumoto and N. Chatani, *J. Am. Chem. Soc.*, 2014, **136**, 15509; (d) A. Yokota, Y. Aihara and N. Chatani, *J. Org. Chem.*, 2014, **79**, 11922; (e) M. Iyanaga, Y. Aihara and N. Chatani, *J. Org. Chem.*, 2014, **79**, 11933; (f) Y. Aihara, J. Wülbern and N. Chatani, *Bull. Chem. Soc. Jpn.*, 2015, **88**, 438; (g) A. Yokota and N. Chatani, *Chem. Lett.*, 2015, **44**, 902; (h) T. Kubo, Y. Aihara and N. Chatani, *Chem. Lett.*, 2015, **44**, 1365; (i) L. C. Misal Castro, A. Obata, Y. Aihara and N. Chatani, *Chem.–Eur. J.*, 2016, **22**, 1362; (j) T. Uemura, M. Yamaguchi and N. Chatani, *Angew. Chem., Int. Ed.*, 2016, **55**, 3162; (k) T. Kubo and N. Chatani, *Org. Lett.*, 2016, **18**, 1698; (l) Y. Aihara and N. Chatani, *ACS Catal.*, 2016, **6**, 4323; (m) A. Sasagawa, M. Yamaguchi, Y. Ano and N. Chatani, *Isr. J. Chem.*, 2017, **57**, 964.
  - For representative papers reported by other groups, see: (a) X. Wu, Y. Zhao and H. Ge, *J. Am. Chem. Soc.*, 2014, **136**, 1789; (b) W. Song, S. Lackner and L. Ackermann, *Angew. Chem., Int. Ed.*, 2014, **53**, 2477; (c) M. Li, J. Dong, X. Huang, K. Li, Q. Wu, F. Song and J. You, *Chem. Commun.*, 2014, **50**, 3944; (d) X. Cong, Y. Li, Y. Wei and X. Zeng, *Org. Lett.*, 2014, **16**, 3926; (e) X. Wang, R. Qiu, C. Yan, V. P. Reddy, L. Zhu, X. Xu and S.-F. Yin, *Org. Lett.*, 2015, **17**, 1970; (f) X. Wu, Y. Zhao and H. Ge, *J. Am. Chem. Soc.*, 2015, **137**, 4924; (g) X. Ye, J. L. Petersen and X. Shi, *Chem. Commun.*, 2015, **51**, 7863; (h) Y.-J. Liu, Z.-Z. Zhang, S.-Y. Yan, Y.-H. Liu and B.-F. Shi, *Chem. Commun.*, 2015, **51**, 7899; (i) N. Barsu, D. Kalsi and B. Sundararaju, *Chem.–Eur. J.*, 2015, **21**, 9364; (j) M. Sattar, Praveen, C. D. Prasad, A. Verma, S. Kumar and S. Kumar, *Adv. Synth. Catal.*, 2016, **358**, 240; (k) C. Lin, J. Zhang, Z. Chen, Y. Liu, Z. Liu and Y. Zhang, *Adv. Synth. Catal.*, 2016, **358**, 1778; (l) V. G. Landge, C. H. Shewale, G. Jaiswal, M. K. Sahoo, S. P. Midya and E. Balaraman, *Catal. Sci. Technol.*, 2016, **6**, 1946; (m) B. Khan, R. Kant and D. Koley, *Adv. Synth. Catal.*, 2016, **358**, 2352; (n) Z. He and Y. Huang, *ACS Catal.*, 2016, **6**, 7814; (o) F.-X. Luo, Z.-C. Cao, H.-W. Zhao, D. Wang, Y.-F. Zhang, X. Xu and Z.-J. Shi, *Organometallics*, 2017, **36**, 18; (p) M. Iwasaki, N. Miki, Y. Tsuchiya, K. Nakajima and Y. Nishihara, *Org. Lett.*, 2017, **19**, 1092; (q) X. Wang, P. Xie, R. Qiu, L. Zhu, T. Liu, Y. Li, T. Iwasaki, C.-T. Au, X. Xu, Y. Xia, S.-F. Yin and N. Kambe, *Chem. Commun.*, 2017, **53**, 8316; (r) S. Xu, K. Takamatsu, K. Hirano and M. Miura, *Angew. Chem., Int. Ed.*, 2018, **57**, 11797.
  - (a) A. Obata, Y. Ano and N. Chatani, *Chem. Sci.*, 2017, **8**, 6650; (b) K. Yamazaki, A. Obata, A. Sasagawa, Y. Ano and N. Chatani, *Organometallics*, 2019, **38**, 248.
  - H. Shiota, Y. Ano, Y. Aihara, Y. Fukumoto and N. Chatani, *J. Am. Chem. Soc.*, 2011, **133**, 14952.
  - (a) K. W. Bentley, *Nat. Prod. Rep.*, 1992, **9**, 365; (b) J. Zhang, S. Didierlaurent, M. Fortin, D. Lefrançois, E. Uridat and J. P. Vevert, *Bioorg. Med. Chem. Lett.*, 2000, **10**, 1351; (c) Y. Bansal and O. Silakari, *Bioorg. Med. Chem.*, 2012, **20**, 6208; (d) U. H. F. Bunz, J. U. Engelhart, B. D. Lindner and M. Schaffroth, *Angew. Chem., Int. Ed.*, 2013, **52**, 3810; (e) A. Mateo-Alonso, *Chem. Soc. Rev.*, 2014, **43**, 6311; (f) Y. Deng, Y. Xie, K. Zou and X. Ji, *J. Mater. Chem. A*, 2016, **4**, 1144.
  - Ru(II): (a) L. Ackermann, L. Wang and A. V. Lygin, *Chem. Sci.*, 2012, **3**, 177; (b) N. Kavitha, G. Sukumar, V. P. Kumar, P. S. Mainkar and S. Chandrasekhar, *Tetrahedron Lett.*, 2013, **54**, 4198; (c) R. Wang and J. R. Falck, *J. Organomet. Chem.*, 2014, **759**, 33; (d) S. Karthik, J. Ajantha, C. M. Nagaraja, S. Easwaramoorthi and T. Gandhi, *Org. Biomol. Chem.*, 2016, **14**, 10255. Rh(III): (e) N. Umeda, T. Tsurugi, T. Satoh and M. Miura, *Angew. Chem., Int. Ed.*, 2008, **47**, 4019; (f) K. Morimoto, K. Hirano, T. Satoh and M. Miura, *Org. Lett.*, 2010, **12**, 2068; (g) X. Li and M. Zhao, *J. Org. Chem.*, 2011, **76**, 8530; (h) H. Sun, C. Wang, Y.-F. Yang, P. Chen, Y.-D. Wu, X. Zhang and Y. Huang, *J. Org. Chem.*, 2014, **79**, 11863; (i) J. M. Villar, J. Suárez, J. A. Varela and C. Saá, *Org. Lett.*, 2017, **19**, 1702. Ru(II) and Rh(III): (j) A. G. Algarra, Q. B. Cross, D. L. Davies, Q. Khamker, S. A. Macgregor, C. L. McMullin and K. Singh, *J. Org. Chem.*, 2014, **79**, 1954; (k) L. Zheng and



- R. Hua, *J. Org. Chem.*, 2014, **79**, 3930. Co(III): (l) P. K. Dutta and S. Sen, *Eur. J. Org. Chem.*, 2018, 5512.
- 15 J. Guihaumé, S. Halbert, O. Eisenstein and R. N. Perutz, *Organometallics*, 2012, **31**, 1300.
- 16 An LLHT mechanism is proposed to be involved in C–H functionalizations in which other first-row transition metal complexes, such as Ni, Mn, Fe, and Co. For recent papers in which LLHT mechanism is proposed, see: (a) A. J. Nett, W. Zhao, P. M. Zimmerman and J. Montgomery, *J. Am. Chem. Soc.*, 2015, **137**, 7636; (b) J. S. Bair, Y. Schramm, A. G. Sergeev, E. Clot, O. Eisenstein and J. F. Hartwig, *J. Am. Chem. Soc.*, 2014, **136**, 13098; (c) L.-J. Xiao, X.-N. Fu, M.-J. Zhou, J.-H. Xie, L.-X. Wang, X.-F. Xu and Q.-L. Zhou, *J. Am. Chem. Soc.*, 2016, **138**, 2957; (d) S. Tang, O. Eisenstein, Y. Nakao and S. Sakaki, *Organometallics*, 2017, **36**, 2761; (e) A. J. Nett, J. Montgomery and P. M. Zimmerman, *ACS Catal.*, 2017, **7**, 7352; (f) S. Nakanowatari, T. Müller, J. C. A. Oliveira and L. Ackermann, *Angew. Chem., Int. Ed.*, 2017, **56**, 15891; (g) J. Diesel, A. M. Finogenova and N. Cramer, *J. Am. Chem. Soc.*, 2018, **140**, 4489.
- 17 Details of the energy profile for the left path are shown in the ESI (Scheme S1†).

